NRC Publications Archive
Archives des publications du CNRC

The contribution of larval zebrafish transcriptomics to chemical risk assessment

Morash, Michael G.; Kirzinger, Morgan W.; Achenbach, J. C.; Venkatachalam, Ananda B.; Cooper, Joëlle Pinsonnault; Ratzlaff, Deborah E.; Woodland, Cindy L. A.; Ellis, Lee D.

This publication could be one of several versions: author's original, accepted manuscript or the publisher's version. / La version de cette publication peut être l'une des suivantes : la version prépublication de l'auteur, la version acceptée du manuscrit ou la version de l'éditeur.
For the publisher's version, please access the DOI link below./ Pour consulter la version de l'éditeur, utilisez le lien DOI ci-dessous.

Publisher's version / Version de l'éditeur:
https://doi.org/10.1016/j.yrtph.2023.105336
Regulatory Toxicology and Pharmacology, 138, C, pp. 1-8, 2023-01-13

NRC Publications Archive Record / Notice des Archives des publications du CNRC :
https://nrc-publications.canada.ca/eng/view/object/?id=7e964d46-b61b-48fe-be99-6108ae7d3703
https://publications-cnrc.canada.ca/fra/voir/objet/?id=7e964d46-b61b-48fe-be99-6108ae7d3703

Access and use of this website and the material on it are subject to the Terms and Conditions set forth at
https://nrc-publications.canada.ca/eng/copyright
READ THESE TERMS AND CONDITIONS CAREFULLY BEFORE USING THIS WEBSITE.

L'accès à ce site Web et l'utilisation de son contenu sont assujettis aux conditions présentées dans le site
https://publications-cnrc.canada.ca/fra/droits
LISEZ CES CONDITIONS ATTENTIVEMENT AVANT D'UTILISER CE SITE WEB.

Questions? Contact the NRC Publications Archive team at
PublicationsArchive-ArchivesPublications@nrc-cnrc.gc.ca. If you wish to email the authors directly, please see the first page of the publication for their contact information.

Vous avez des questions? Nous pouvons vous aider. Pour communiquer directement avec un auteur, consultez la première page de la revue dans laquelle son article a été publié afin de trouver ses coordonnées. Si vous n'arrivez pas à les repérer, communiquez avec nous à PublicationsArchive-ArchivesPublications@nrc-cnrc.gc.ca.

National Research Council Canada
Conseil national de recherches Canada

Regulatory Toxicology and Pharmacology 138 (2023) 105336

Contents lists available at ScienceDirect

Regulatory Toxicology and Pharmacology

journal homepage: www.elsevier.com/locate/yrtph

The contribution of larval zebrafish transcriptomics to chemical risk assessment

Michael G. Morash [a,*], Morgan W. Kirzinger [b], J.C. Achenbach [a], Ananda B. Venkatachalam [a], Joëlle Pinsonnault Cooper [c], Deborah E. Ratzlaff [c], Cindy L.A. Woodland [c], Lee D. Ellis [a]

[a] Aquatic and Crop Resource Development, National Research Council of Canada, Halifax, NS B3H 3Z1, Canada
[b] Aquatic and Crop Resource Development, National Research Council of Canada, Saskatoon, SK S7N 0W9, Canada
[c] New Substances Assessment Control Bureau, Health Canada, Ottawa, ON K1A 0K9, Canada

ARTICLE INFO

Handling Editor: Martin Van den berg

Keywords:
Raloxifene
Resorcinol
Transcriptomics
RNAseq
Zebrafish

ABSTRACT

In Canada, the Canadian Environmental Protection Act (1999) requires human health and environmental risk assessments be conducted for new substances prior to their manufacture or import. While this toxicity data is historically obtained using rodents, in response to the international effort to eliminate animal testing, Health Canada is collaborating with the National Research Council (NRC) of Canada to develop a New Approach Method by refining existing NRC zebrafish models. The embryo/larval zebrafish model evaluates systemic (whole body) general toxicity which is currently unachievable with cell-based testing. The model is strengthened using behavioral, toxicokinetic and transcriptomic responses to assess non-visible indicators of toxicity following chemical exposure at sub-phenotypic concentrations. In this paper, the predictive power of zebrafish transcriptomics is demonstrated using two chemicals; Raloxifene and Resorcinol. Raloxifene exposure produced darkening of the liver and malformation of the nose/mandible, while Resorcinol exposure produced increased locomotor activity. Transcriptomic analysis correlated differentially expressed genes with the phenotypic effects and benchmark dose calculations determined that the transcriptomic Point of Departure (POD) occurred at subphenotypic concentrations. Correlating gene expression with apical (phenotypic) effects strengthens confidence in evaluation of chemical toxicity, thereby demonstrating the significant advancement that the larval zebrafish transcriptomics model represents in chemical risk assessment.

1. Introduction

Quantitative chemical risk assessment is critical for ensuring maximal protection of human health and the environment. The need for accurate and predictive toxicological data used to conduct these assessments is increasing as a result of the continued increase in the number of new chemicals. Simultaneously, the development of Integrated Approaches for Testing and Assessment (IATAs) seeks to combine various toxicological data sets (*in silico*, *ex vivo*, *in vitro*) to perform risk assessments in a manner that reduces the need for animal testing (OECD, 2020). This, combined with the international momentum to eliminate animal testing in chemical risk assessment, necessitates adoption of the 3 R's of refining, reducing and/or replacing the use of animals in toxicity testing, and a subsequent move away from higher animal testing (Leist et al., 2012; Van Norman, 2019). As such, many regulatory agencies are developing new alternative animal models for toxicity testing (Dolgin, 2010; Kavlock et al., 2018; Scholz et al., 2013). The development of these New Approach Methods (NAMs) aims to maximize the information obtained through progressive experimentation on less complex biological systems (eg. cell lines), before progressing to higher organisms. Because zebrafish larvae are not considered animals until they are 5–7 days post-fertilization, this toxicity testing model aligns well with the 3 R's and is poised to become a regulated, entry level step in the risk assessment process (Caballero and Candiracci, 2018; Kanungo et al.,

Abbreviations: BMD, Benchmark Dose; DEG, Differentially Expressed Gene; GO, Gene Ontology; HC, Health Canada; Hpf, Hours post-fertilization; NAM, New Approach Method; NRC, National Research Council of Canada; POD, Point of Departure.

* Corresponding author.
E-mail addresses: michael.morash@nrc-cnrc.gc.ca (M.G. Morash), Morgan.Kirzinger@nrc-cnrc.gc.ca (M.W. Kirzinger), John.Achenbach@nrc-cnrc.gc.ca (J.C. Achenbach), Ananda.Venkatachalam@nrc-cnrc.gc.ca (A.B. Venkatachalam), joelle.pinsonnaultcooper@hc-sc.gc.ca (J.P. Cooper), deborah.ratzlaff@hc-sc.gc.ca (D.E. Ratzlaff), cindy.woodland@hc-sc.gc.ca (C.L.A. Woodland), Lee.Ellis@nrc-cnrc.gc.ca (L.D. Ellis).

https://doi.org/10.1016/j.yrtph.2023.105336
Received 4 November 2022; Received in revised form 22 December 2022; Accepted 10 January 2023
Available online 13 January 2023
0273-2300/Crown Copyright © 2023 Published by Elsevier Inc. This is an open access article under the CC BY-NC license (http://creativecommons.org/licenses/by-nc/4.0/).

2014; Rodrigues et al., 2020; Sukardi et al., 2011).

Ultimately, the goal of toxicological testing is to relate a chemical concentration with a particular adverse effect, and to extrapolate those data to humans and/or their environment (Hayes et al., 2020). While regulatory risk assessments have historically relied on Point of Departure (POD) data from mammalian toxicity studies to evaluate risk to human health (Izadi et al., 2012), the zebrafish is now an established model for predicting chemical effects in humans in drug development (Cassar et al., 2019) and toxicant screening (Lai et al., 2021). In mammalian toxicity studies, POD determination is typically based on no observed (adverse) effect level (NO(A)EL) and lowest observed adverse effect level (LO(A)EL). However, NO(A)EL and LO(A)EL data generated are heavily dependent on the experimental conditions (eg. limited explicitly to the specific concentration/dose tested) and the presence of overt phenotypes (i.e. the inability to detect sub-phenotypic effects) (Hayes et al., 2020). Benchmark Dose (BMD) modelling, which calculates the concentration of chemical that corresponds to a particular adverse effect, has been shown to overcome a number of limitations of these methods (Hayes et al., 2020; Izadi et al., 2012). More specifically, transcriptomic BMD calculations have been shown to provide PODs that are more sensitive than the traditional apical endpoints in mammals (Farmahin et al., 2017; Johnson et al., 2020; LaRocca et al., 2020) and recently the use of transcriptomics in chemical risk assessment to supplement and/or replace apical endpoint testing has been proposed (Johnson et al., 2022). Similarly, transcriptomic PODs are predictive of apical endpoints in fish species, including zebrafish (Page-Lariviere et al., 2019), which can be leveraged for human health risk assessment, particularly given zebrafish gene homology with humans. A transcriptomic approach to risk assessment offers two significant advantages to other methods; it allows for the assessment of molecular pathways that do not produce visually quantifiable phenotypes, and it may provide a more sensitive model where gene expression perturbations precede phenotypic alterations (sub-phenotypic), while still predicting the underlying mechanism of action (MOA). The second advantage is significant in the context of risk assessments of chemicals that can exert adverse effects, such as hormonal effects, at environmentally relevant levels prior to manifestation as an observable apical endocrine-disrupting effect. This is significant as it allows for a health-based chemical risk assessment without conducting studies in higher animals for potential endocrine effects.

In this report, we demonstrate the potential of the zebrafish larval transcriptomic approach as a NAM for toxicity testing using two drugs: Raloxifene and Resorcinol. Both chemicals produced phenotypic toxicological endpoints that coincided with differential gene expression changes. The benchmark dose derived POD revealed that these gene expression changes occurred at lower concentrations than the phenotypic effects themselves. We also identified a number of other pathways affected where phenotypic assessment was not possible, including perturbation of endocrine related systems, which may represent as of yet unidentified toxicities. In conclusion, the transcriptomic approach described herein enhances the sensitivity and predictability of the embryo/larval zebrafish assay, and is poised to become a supplement to current non-mammalian risk assessment methodologies.

2. Materials and methods

2.1. Chemicals

Raloxifene-HCl (CAS# 82,640-04-8, purity >99%), Resorcinol (CAS# 108-46-3, purity ≥99%) and DMSO (Cat#D8418, purity ≥99%) were all purchased from Sigma-Aldrich (Oakville, ON, CAN). Raloxifene-HCl and Resorcinol were dissolved in DMSO at a stock concentration of 200 mM. All stocks were stored at −20 °C.

2.2. Animal husbandry

All zebrafish larvae used were obtained from breeding of wild-type AB/Tub hybrids, created in-house from adult AB and Tuebingen Long Fin adults acquired from the Zebrafish International Resource Center (ZIRC – Eugene, Oregon, USA). Age-matched embryos were sorted for fertilization at roughly 4 h post-fertilization (hpf) in E3 media (5 mM NaCl, 0.17 mM KCl, 0.33 mM $CaCl_2–2H_2O$, 0.33 mM $MgSO_4–7H_2O$) in 10 × 150 mm disposable polystyrene Petri dishes, were transferred to Pentair Aquatic Ecosystem (Apopka, FL, USA) nursery baskets (maximum 200 embryos per basket) residing in a 3-L tank in a ZebTec Recirculation Water Treatment System (Tecniplast USA, Easton, PA, USA) and raised until 72 hpf. The water temperature within this system was maintained at 28.5 ± 0.5 °C and the room housing the tank was kept on a 14:10 light: dark cycle. All adult zebrafish husbandry and breeding was in accordance with the Canadian Council of Animal Care (CCAC) guidelines.

2.3. Chemical larval exposures

72 hpf larvae were placed individually into wells of a 96-well round bottom microtiter plate in 270 μl of a HEPES buffered E3 (HE3) medium (5 mM NaCl, 0.17 mM KCl, 0.33 mM $CaCl_2–2H_2O$, 0.33 mM $MgSO_4–7H_2O$, 10 mM HEPES, pH 7.2) followed by the addition of 30 μl of a 10 X working stock of test chemical into each well (12 wells per exposure concentration) when the larvae were 72 ± 0.5 hpf. 10 X working stocks were prepared by diluting 200 mM stock into HE3 with a final DMSO concentration of 5% (Raloxifene) or 10% (Resorcinol). DMSO alone was used as a Carrier Control (CC). Plates were sealed and incubated at 28.5 °C for 48 h. At 96 and 120 hpf larvae were manually scored for altered phenotypes and lethality as described (Achenbach et al., 2020).

2.4. Behavioral and toxicity testing

Prior to 120 hpf scoring, larval behavior was analyzed using DanioVision larval tracking systems with EthoVision XT14/15 software (Noldus Information Technology Inc., Virginia, USA). Total distance travelled was captured every second using an infrared camera, and grouped in 1 min bins. Background was removed using dynamic subtraction. Experiments were conducted at 28.5 °C over 60 min with the first 30 min under lighted conditions (15 μmol m-2 s-1), followed by alternating 5-min dark/light cycles. Two metrics of behavior were used: The average total distance per minute over the first 30 min light phase, and the difference in average distance travelled between the first 5 min dark cycle and its preceding 5 min light phase. Each larvae represents an independent measurement. Any larvae that were dead or displayed phenotypic abnormalities were removed from analysis. 12 larvae were used in each experimental concentration, and at least 3 replicates of each concentration were performed. Statistical significance was calculated using One-way ANOVA with a Bonferroni post hoc test.

2.5. Larval imaging

Larvae were exposed to each chemical as described above. At 120 hpf, larvae were anesthetized with 130 μg/ml of Tricaine and transferred to 1.5% methylcellulose. All images were acquired using an EVOS XL Core Imaging System (Fisher Scientific, Ottawa, Ontario, CAN).

2.6. Transcriptomics sampling

Experimental set up was described as above. Compounds were assayed at their previously calculated EC_{20} value (Raloxifene-HCl 20.1 μM and Resorcinol 405 μM) and at four further subsequent 10-fold dilutions. EC_{20} values (the concentration at which 20% of larvae displayed phenotypic abnormalities or death) were calculated from previously published results (Achenbach et al., 2020). At least 24 larvae were exposed at each concentration of test substance in order to ensure that 20 living larvae could be collected at the 120 hpf time point (114 h of exposure). Plates were sealed and incubated at 28.5 °C for 48 h. At 120 hpf larvae were manually scored for altered phenotypes. Phenotypically normal larvae were collected into Corning Netwell baskets and rinsed five times in vehicle control media. They were washed once in Milli-Q type I water and collected into microcentrifuge tubes. The residual water was removed and the larvae flash frozen on dry ice and stored at −80 °C before total RNA extraction.

2.7. RNA isolation and sequencing

Total RNA was extracted from each sample of 20 larvae using the Norgen BioTek Corp Total RNA Purification kit (Norgen Cat#17200, Thorold, ON, Canada) with the optional RNase-Free DNase I kit (Norgen Cat#25710, Thorold, ON, CAN). Total RNA was quantitated by absorption spectroscopy with an average recovery of 234 ng/μl (range: 131–421 ng/μl) and 207 ng/μl (range: 102–493 ng/μl) for Raloxifene and Resorcinol respectively. RNA integrity was confirmed on an Agilent Bioanalyzer using an Agilent RNA 6000 pico kit (Agilent Cat# 5067–1513, Santa Clara, CA, USA) with RIN values for these samples averaging 8.7. Sequencing libraries were prepared using the Illumina Truseq Stranded mRNA kit (Illumina Cat# 20020595, San Diego, CA, USA) using 1 μg of total RNA and sequenced on an Illumina Hiseq 2500 using High Output V4 2 × 125bp chemistry. Library sizes averaged ~15 M reads per sample.

2.8. Sequence alignment and quantification

Sequencing reads were aligned to the zebrafish genome (GRCz11) using Spliced Transcripts Alignment to a Reference (STAR) under default parameters (Dobin et al., 2013). Supporting Information Table 1 outlines key statistics regarding alignment results. Sequencing data have been uploaded to the NCBI Gene Expression Omnibus repository (GSE207739).

2.9. Differential gene expression (DEG) analysis

Raw sequencing read files were trimmed using cutadapt (Martin, 2011). Fastqc (Andrews, 2010) was used to analyze the quality of the reads before and after trimming, and STAR aligner (Dobin et al., 2013; Dobin and Gingeras, 2015) using quant mode was used to calculate the reads per gene. Raw read per gene counts from STAR were formatted into a matrix (gene x sample) and imported into DESeq2 (Love et al., 2014) for all differential gene expression analyses and pairwise comparisons. An adjusted p-value (padj, q) false discovery rate (FDR) of 0.05 (Benjamini and Hochberg) was used as the initial cutoff value, followed by an additional cutoff using a log fold change (LFC) of 1.5 (log2 = 0.585). Results of pairwise comparisons of Carrier control vs EC_{20} are shown in Supporting Information files 1 and 2.

2.10. Gene ontology (GO) analysis

DEGs (LFC >1.5, q < 0.05) identified above were used for GO term analysis using the online tool gprofiler (https://biit.cs.ut.ee/gprofiler/gost) using default *D. rerio* settings, except "all known genes" option and the Benjamini-Hochberg FDR of 0.05 were used. Results from GO-terms, Reactome and the Kyoto Encyclopedia of Genes and Genomes (KEGG) pathways are reported herein, and full lists are included in Supporting Information files 3 and 4.

2.11. Benchmark dose curve fitting

Normalized quantile data for all genes from DEseq2 was imported into BMDExpress 2.3 (Phillips et al., 2019) and principal component analysis run as an initial evaluation of the replicates/samples. The workflow for all transcriptomic analysis was based on the work done by (Page-Lariviere et al., 2019). Imported data was prefiltered using the Williams Trend Test with a cut-off value of 1.5 fold. Filtered genes were then subjected to BMD dose-response curve fitting using all fitting models (Hill, Power, Linear, Exp 2, Exp 3, Exp 4, Exp 5, Poly 2, Poly 3 and Poly 4). Fitted curves were then subjected to a post-filtering to remove poorly fitted curves: a ratio of upper and lower confidence intervals greater than 40 (BMDU/BMDL >40), a BMD greater than the highest concentration tested, and a BMD lower than 10-fold below the lowest tested concentration. Genes were then subjected to GO analysis using the same post-filtering criteria as those described for BMD cut-off.

2.12. Transcriptomic Point of Departure calculation and interpretation

Two approaches were used to calculate the concentration of chemical required to produce a transcriptomic POD. In the first, post-filtered BMD values and their associated genes were exported into a spreadsheet, sorted in ascending order, and the 10th percentile value calculated. This concentration is expressed as the transcriptomic POD (10th). The same post-filtered BMDs were also analyzed for modes and antimodes using a custom written R script (Page-Lariviere et al., 2019) which identifies local modes based on the distribution of kernel density. Graphs showing these modes are shown in Supporting Information Fig. 1. The first mode (i.e. the first mode identified at the lowest concentration) is termed the transcriptomic POD (mode). Genes that comprised the first mode for each compound were then subjected to GO analysis using the same post-filtering criteria as those described above.

3. Results

3.1. Phenotypic toxicity assessments

The phenotypic and behavioral EC_{50} and LC_{50} values of both compounds were previously determined (Achenbach et al., 2020). In order to minimize the effects of general toxicity on downstream transcriptomic analysis, we calculated the EC_{20} values from the previously published data, and assessed toxicity near these values (Raloxifene = 20.1 μM, 95% CI 10.0–24.8 μM, Resorcinol = 405 μM, 95% CI 146–734 μM). At 25 μM, Raloxifene exposure led to significant darkening of the liver, and necrosis of the mandible (Fig. 1E) and nose pits (Fig. 1F). At 15 μM, liver darkening was also noted. (Fig. 1 panels C and D). No

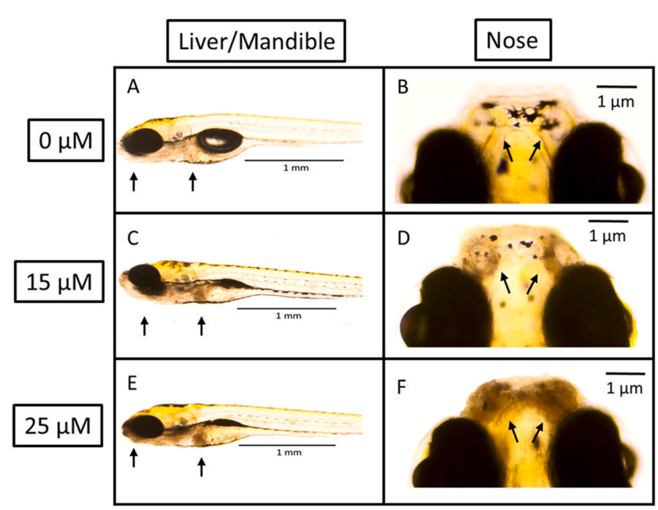

Fig. 1. Phenotypic assessment of Raloxifene toxicity. Raloxifene induced necrosis of the mandible and darkening of the liver at 15 and 25 μM (arrows, panels C and E), when compared to DMSO carrier control (panel A). Necrosis was also apparent in the nose pits (panels D and F).

dose-dependent effect on behaviour was observed at these concentrations (data not shown).

The predominant effect of resorcinol exposure was altered swimming activity. Behavioral analysis confirmed that at increased concentrations, both baseline activity (30 min light) and the larval startle response (First light/dark transition) were initially increased followed by a decrease at the highest concentrations tested (Fig. 2). At 1000 and 2000 μM, larvae no longer responded to the light to dark transition, but retained their constant movement pattern. No consistent phenotypic effects were observed at these concentrations.

3.2. Transcriptomic profiling of chemical exposure

Differential gene expression was initially determined by pairwise comparison of the EC_{20}-treated and DMSO carrier control samples using DEseq2. Statistically significant DEGs were identified using two cut-off criteria, a fold-change of 1.5, and a $q < 0.05$. Raloxifene (20.1 μM) and Resorcinol (405 μM) exposure produced 174 and 79 DEGs respectively. Both compounds displayed an even distribution of up and down-regulated genes.

As expected, a number of DEGs and GO-terms related to the observed phenotypes were identified (Table 1). The most statistically significant GO pathways identified for Raloxifene were populated largely by down-regulated DEGs and were related to olfactory and liver function, which were expected given the necrosis seen in the nose pit/mandible areas and the liver. Interestingly several GO-terms were related to immune function, which is not an observable phenotype. For Resorcinol, the GO analysis revealed that light-sensory pathways were significantly affected with several DEGs (~15% of all DEGs detected) implicated in phototransduction. Specifically a number of GO-terms implicated in guanylate cyclase regulation, cGMP phosphodiesterase activity, light perception and structural components of sensory cells were identified (Table 1). The related GO-terms contained a range of behavioral and locomotive functions, which could be related to altered behaviour observed in Resorcinol treated larvae. Interestingly genes related to thyroid function and maturation (thyroid hormone receptor alpha (a) and iodothyronine deiodinase 3b) were also differentially expressed, suggesting that Resorcinol may be exerting goitrogenic effects (supplemental file 2).

3.3. Benchmark dose (BMD) and transcriptomic Point of Departure (POD) calculations

We used BMD to model gene expression changes of differentially expressed genes over a wide range of subphenotypic dilutions. To determine the transcriptomic POD for each compound, the list of filtered BMDs is analyzed using two previously published approaches, the 10th percentile and the Mode approach (Page-Lariviere et al., 2019) and both approaches yielded similar values (Table 2). All calculated transcriptomic POD values were lower than the EC_{20} phenotype based calculations. In each case, the POD mode and 10th were similar because in both cases, the top 10 percent of DEGs each made up their own mode grouping.

The genes which make up the first mode cluster represent the most sensitive genes (i.e. those whose expression is modulated at the lowest concentrations). To determine whether these represented specific pathways, the genes making up that mode cluster were subjected to GO analysis. For Raloxifene, BMDs in the first mode corresponded to the same olfactory and odorant GO terms as seen in the pairwise comparisons (Table 3), although the BMD method identified some different member genes. Similarly, the mode genes for Resorcinol identified the guanylate cyclase related GO-terms. Therefore the mode clusters of genes are able to identify the most sensitive pathways.

4. Discussion

The goal of NAMs is to develop robust data sets that have optimal sensitivity and specificity in the identification of toxicological endpoints that can be used to predict risk to human health and the environment. In support of that goal, the zebrafish embryo-larval toxicity testing using apical endpoints has been identified as a valuable NAM for chemical risk assessment (Rodrigues et al., 2020; Scholz et al., 2013). The goal of this work is to demonstrate the potential of transcriptomics to supplement the embryo-larval zebrafish model by providing enhanced sensitivity and predictability to these developing models. In the current study, we expanded upon previously developed zebrafish embryo-larval models (Achenbach et al., 2020), which have focused on phenotypic profiling, to include transcriptomic assays. The initial goal of developing a transcriptomic approach to toxicity testing is to identify the changes in gene expression underlying ultimate apical adverse effects, and to identify

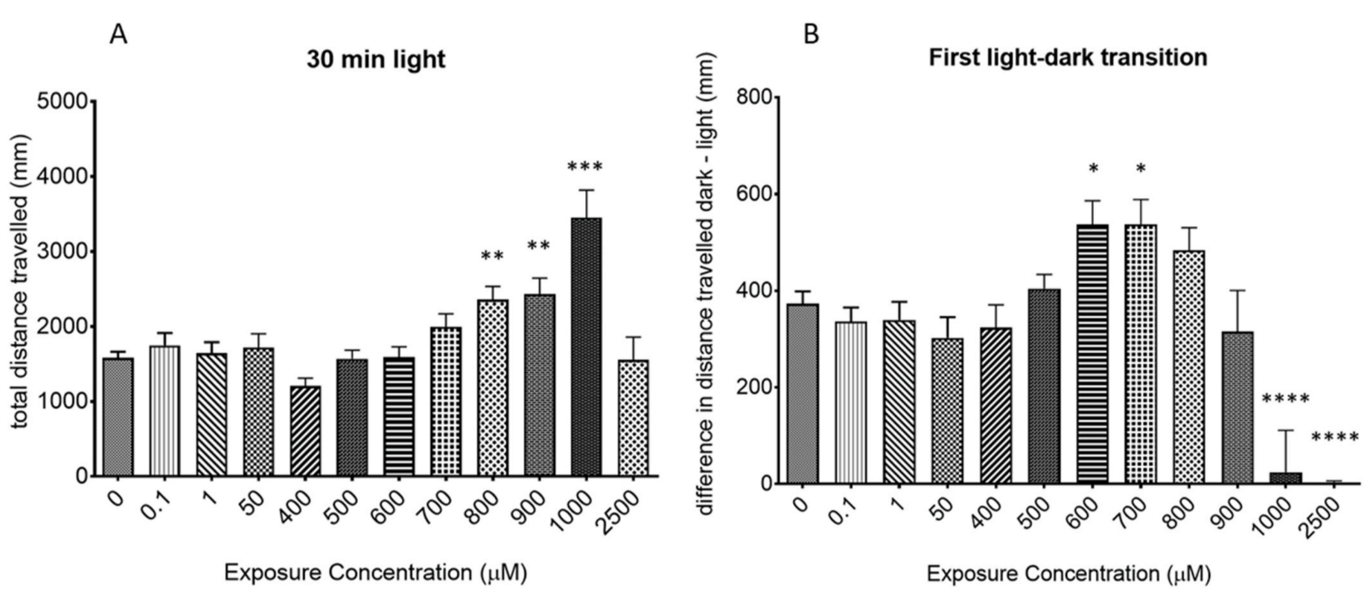

Fig. 2. Behavioral assessment of Resorcinol toxicity. A - Baseline activity was measured over the first 30 min in the light by analyzing the distance travelled (mm). B - The startle response was measured by subtracting the preceding 5 min of activity from that activity change induced by the light to dark transition. *, **, ***, **** = $p < 0.05, 0.01, 0.001, 0.0001$, ANOVA, Bonferroni multiple comparison.

Table 1
GO-terms identified by transcriptomics related to observed phenotypes induced by Raloxifene and Resorcinol. Go-terms and their numbers are listed, as well as representative (example) genes, and their description that populated these GO-terms. Also included are GO-terms related to the initial GO-terms identified. MF = Molecular Function, BP = Biological Process, CC = Cellular Component, REAC = Reactome. FA = Fatty acid, OR = Odorant Receptor. Genes in green were upregulated, genes in red downregulated.

Raloxifene				
GO-term description	GO-term/REAC	Example Gene	Description	Related GO-terms
Olfaction				
Olfactory receptor activity	GO:0004984 (MF)	or115-11	OR Family F (115/11)	GO:0021559 (Trigeminal nerve development)
Odorant binding	GO:0005549 (MF)	or103-5	OR Family C (103/5)	GO:0071683 (Sensory dendrite)
G protein-coupled receptor activity	GO:0004930 (MF)	or111-1	OR Family D (111/1)	GO:0042048 (Olfactory behavior)
Detection of chemical stimulus (perception of smell)	GO:0050911 (BP)	or119-2	OR Family F (119/2)	GO:0021630 (Olfactory nerve maturation)
Sensory perception of smell	GO:0007608 (BP)	or116-2	OR Family F (116/2)	
Detection of chemical stimulus (perception)	GO:0050907 (BP)	zgc:152857	zgc:152857	
Detection of chemical stimulus	GO:0009593 (BP)	or128-5	OR Family E (128/5)	
Sensory perception of chemical stimulus	GO:0007606 (BP)			
Detection of stimulus involved in sensory perception	GO:0050906 (BP)			
Liver Function				
Endopeptidase regulator activity	GO:0061135 (MF)	cetp	Cholesteryl ester transfer	GO:0032384 (Cholesterol transport)
Fatty acid binding	GO:0005504 (MF)	fabp1b.1	FA binding protein 1 b	GO:0010872 (Cholesterol transport)
Phosphatidylcholine binding	GO:0031210 (MF)	lipg	Lipase	GO:0015908 (FA transport)
Hydroxymethylglutaryl-CoA synthase activity	GO:0004421 (MF)	fabp6	FA binding protein 6	GO:0055088 (Lipid homeostasis)
Triglyceride binding	GO:0017129 (MF)			GO:0034375 (HDL particle)
HDL remodeling	R-DRE-8964058 (REAC)			GO:0034380 (HDL particle)
Triglyceride catabolism	R-DRE-163560 (REAC)			GO:0010142 (Farnesyl biosynthetic process)
Plasma lipoprotein remodeling	R-DRE-8963899 (REAC)			GO:0010890 (Sequestering of triglyceride)
Triglyceride metabolism	R-DRE-8979227 (REAC)			
Immune System				
CXCR chemokine receptor binding	GO:0045236 (MF)	cxcl18 b	CXC chemokine ligand 18 b	GO:0002870 (T cell anergy)
Chemokine activity	GO:0008009 (MF)	cxcl19	CXC chemokine ligand 19	GO:0002669 (T cell anergy)
Chemokine receptor binding	GO:0042379 (MF)	cxcl18a.1	CXC chemokine ligand 18a	GO:0048247 (Lymphocyte chemotaxis)
Detection of stimulus	GO:0051606 (BP)	s100z	S100 Ca Bind Protein Z	GO:0001768 (T cell polarity)
Antimicrobial humoral immune response	GO:0061844 (BP)	ahsg2	alpha-2-HS-glycoprotein 2	GO:0045954 (NK cell)
Neutrophil degranulation	R-DRE-6798695 (REAC)	AL954146.1	Trypsin I–P1-like	GO:2001185 (T-cell)
Innate Immune System	R-DRE-168249 (REAC)			GO:0019731 (antibacterial humoral response)
Immune System	R-DRE-168256 (REAC)			GO:2001185 (innate humoral response)
Antimicrobial peptides	R-DRE-6803157 (REAC)			

Resorcinol				
GO-term description	GO-term/REAC	Example Gene	Description	Related GO-terms
GO:MF				
Guanylate cyclase activator activity	GO:0030250	si:ch211-103a14.5	si:ch211-103a14.5	GO:0043327 (Chemotaxis)
Cyclase activator activity	GO:0010853	guca1d	Guanylate cyclase activator 1 d	GO:2000305 (Photoreceptor axon guidance)
Calcium sensitive guanylate cyclase activator activity	GO:0008048	guca1e	Guanylate cyclase activator 1e	GO:0007602 (Phototransduction)
Guanylate cyclase regulator activity	GO:0030249	pde6ha	Phosphodiesterase 6H, paralog a	GO:0001917 (Photoreceptor inner segment)
Cyclase regulator activity	GO:0010851	si:ch211-256m1.8	si:ch211-256m1.8	
3′,5′-cyclic-GMP phosphodiesterase activity	GO:0047555			
cGMP binding	GO:0030553			
GO:BP				
Visual perception	GO:0007601	opn1mw2	Opsin 1, med.-wave-sensitive, 2	GO:0007626 (Locomotory behaviour)
Sensory perception of light stimulus	GO:0050953	si:ch211-103a14.5	si:ch211-103a14.5	GO:0009416 (Response to light stimulus)
Positive regulation of guanylate cyclase activity	GO:0031284	pde6ha guca1e	Phosphodiesterase 6H, paralog a Guanylate cyclase activator 1e	GO:0060041 (Retina development) GO:0008344 (Adult locomotory behaviour) GO:0050957 (Equilibrioception)
GO:CC				
photoreceptor outer segment	GO:0001750	si:ch211-103a14.5	si:ch211-103a14.5	GO:0007628 (Adult walking behaviour)
photoreceptor cell cilium	GO:0097733	pde6ha guca1e	Phosphodiesterase 6H, paralog a Guanylate cyclase activator 1e	GO:0042756 (Drinking behaviour) GO:1903998 (Eating behaviour)
KEGG/REAC				
Phototransduction	KEGG:04744	si:ch211-103a14.5	si:ch211-103a14.5	
Regulation of the phototransduction cascade	R-DRE-2514859	guca1d	Guanylate cyclase activator 1 d	
The phototransduction cascade	R-DRE-2514856	rbp1.2	Retinol binding protein 1, cellular	
Visual phototransduction		grk7b	GPCR kinase 7 b	

(continued on next page)

Table 1 (*continued*)

Resorcinol				
GO-term description	GO-term/REAC	Example Gene	Description	Related GO-terms
Sensory Perception	R-DRE-2187338 R-DRE-9709957	opn1mw2	Opsin 1, med.-wave-sensitive, 2	
		guca1e	Guanylate cyclase activator 1e	

Table 2
Comparison of EC_{20} values. The transcriptomic POD was calculated using the 10th percentile and the 1st mode techniques.

	Raloxifene	Resorcinol
EC_{20}	20.1 μM	405 μM
Transcriptomic POD (10th)	1.82 μM	2.94 μM
Transcriptomic POD (mode)	1.95 μM	2.82 μM

Table 3
GO-term analysis of genes identified from POD (mode) analysis. DEGs identified from the 1st mode were assessed for GO-term function, and the benchmark dose for genes populating those terms are shown. See Table 1 for abbreviations.

Raloxifene				
GO-term description	GO-term/ REAC	Example Gene	Description	BMD (μM)
Olfaction				
Olfactory receptor activity	GO:0004984 (MF)	or111-11	OR Family D (111/11)	1.81
Odorant binding	GO:0005549 (MF)	or125-5	OR Family E (125/5)	2.15
Detection of chemical stimulus (perception of smell)	GO:0050911 (BP)	or115-15	OR Family F (115/15)	2.15
Sensory perception of smell	GO:0007608 (BP)	or115-12	OR Family F (115/12)	2.32
Detection of chemical stimulus (perception)	GO:0050907 (BP)	or116-2	OR Family F (116/2)	4.36
Detection of chemical stimulus	GO:0009593 (BP)			
Resorcinol				
GO-term description	GO-term/ REAC	Example Gene	Description	BMD (μM)
Photoreceptor/transduction				
Guanylate cyclase activator activity	GO:0030250 (MF)	si:ch211-103a14.5	si:ch211-103a14.5	1.59
Cyclase activator activity	GO:0010853 (MF)	guca1d	Guanylate cyclase activator 1 d	2.83
Calcium sensitive guanylate cyclase activator activity	GO:0008048 (MF)	opn1mw2	Opsin 1, med.-wave-sensitive, 2	2.43
Guanylate cyclase regulator activity	GO:0030249 (MF)			
Cyclase regulator activity	GO:0010851 (MF)			

changes in systems that do not produce overt phenotypes. In addition, the analysis of global changes in gene expression provides an unbiased approach that cannot generally be obtained via qPCR or microarray testing (Corchete et al., 2020). In theory, MOA studies also offer a potential chemical fingerprint when assessing the toxicity of unknown/-new chemicals, and attempts to create such systems are showing promise (Schuttler et al., 2017).

A second advantage of the zebrafish transcriptomic approach is the identification of pathways which are highly sensitive to low concentrations of chemical. The assay involves a modification of the BMD calculation model that was adopted by the U.S. EPA as opposed to the previous no observable affect level (NO(A)EL) approach (Davis et al., 2011). BMD modelling is able to return values outside of the test concentrations, is less dependent on dose spacing, and is more robust in studies with low sample numbers (Hayes et al., 2020). Importantly, in some cases, concentration-modelling may not be sufficient to determine mechanistic details, but its utility lies in the sensitivity of transcriptomic PODs to predict chronic apical PODs (Page-Lariviere et al., 2019). The transcriptomic POD for each drug thus allows for the identification of a single concentration at which toxic effects can be demonstrated and enables drugs to be prioritized for further testing. Additionally, transcriptomic dose-response modelling allows for the identification of subsets of genes that display increased sensitivity to the chemical exposure, potentially allowing for earlier detection of markers that indicate the onset of adverse effects.

A significant advantage of the larval zebrafish transcriptomic approach is that it utilizes a whole organism, and so multiple systems can be monitored concurrently. In the current study we observed phenotypic alterations of multiple systems, which were largely associated with predictive changes in gene expression. The necrosis of the lower jaw and nose pits as an olfactory defect is strongly supported by the abundance of olfactory related DEGs and sensory perception GO-terms, and the BMD data demonstrates that this olfactory effect is initiated at dilutions ~10-fold lower than the phenotypic based EC_{20} and represents the first sensitive pathway affected. A similar correlation was observed with the liver darkening induced by Raloxifene which had concomitant gene expression changes in a number of cholesterol and triglyceride biosynthesis pathways, which are indicators of liver dysfunction. Analysis of differential gene expression also identified the activation of a number of steroid hormone biosynthetic pathways. This finding would not have been evident using solely phenotypic observation, demonstrating the power of the model to predict novel non-visible toxicological pathways.

The molecular pathways most significantly affected by Resorcinol exposure involved phototransduction and structural components of the eye. While we did not observe any phenotypic effects on the eye (size, necrosis, etc.), the transcriptomic evidence of Resorcinol toxicity to the visual system in zebrafish is apparent, and the BMD analysis reveals it is a highly sensitive pathway. While the precise relationship between locomotion perturbations and resorcinol induced eye toxicity was not examined here, the relationship between optomotor response and eye toxicity has been well documented (Cassar et al., 2020). As with Raloxifene, the gene expression changes caused by Resorcinol occurred at concentrations well below those required to produce overt phenotypes, further demonstrating the sensitivity of the assay. We also identified differential expression of thyroid hormone receptor genes and iodothyronine deiodinase, which is in line with its potential goitrogenic activity (Hahn et al., 2006; Jarque et al., 2018; Thienpont et al., 2011). Thyroid function has been implicated in eye development (Baumann et al., 2016) and thyroid hormones are known to affect opsin and photoreceptor development in zebrafish (Reider and Connaughton, 2014), and retinal photoreceptor development in higher animals (Jones et al., 2003), however, further studies will be required to identify any causal relationships.

Overall transcriptomics offers the ability to identify perturbed pathways without relying solely on phenotypic readouts. The advantage is significant as phenotypes related to the effects on humans and the environment may not be easily detectable, and gene pathway activation may be more conserved than phenotypic effects. It will therefore be important to correlate the *in vitro* concentration responses seen here to *in vivo* toxicity in humans, which can be done within the regulatory framework of an IATA. Within this framework this zebrafish model can be used in a guided and refined testing approach to generate data to meet entry level (first tier) data requirements, from which the results, and particularly the gene expression results, can be used to select relevant human cell-based/protein-based assays for targeted confirmatory testing in the higher tiers of the IATA (OECD, 2020).

5. Conclusion

In conclusion, we have demonstrated the potential utility of zebrafish transcriptomic markers of toxicity from two compounds, Raloxifene and Resorcinol, for human health and environmental chemical risk assessments. As a New Approach Method the zebrafish model supplemented with a transcriptomics platform allows not only for an evaluation of systemic (whole body) general toxicity, but also provides a sensitive and predictive assessment of toxicity following exposure to chemicals at subphenotypic concentrations. By becoming a part of IATA framework, we believe the larval zebrafish transcriptomic model could become an informative regulatory tool for chemical risk assessment in the international regulatory community, and achieve the goal of replacing, reducing or refining animal testing.

Credit author statement

Michael G. Morash: Methodology, Validation, Formal analysis, Writing – original draft, Visualization. Morgan W. Kirzinger: Software, Validation, Formal analysis, Data curation. J.C. Achenbach: Investigation. Ananda B. Venkatachalam: Investigation. Joëlle Pinsonnault Cooper: Writing – review & editing. Deborah E. Ratzlaff: Writing – review & editing. Cindy L.A. Woodland: Conceptualization, Writing – original draft, Project administration. Lee D. Ellis: Conceptualization, Writing – original draft, Supervision, Project administration.

Ethics statement

All research was approved by the Canadian Council for Animal Care.

Funding information

No external funding was used for the work contained in this manuscript.

Funding body information

This study was funded by the New Substances Assessment and Control Bureau of Health Canada.

Declaration of competing interest

The authors declare that they have no known competing financial interests or personal relationships that could have appeared to influence the work reported in this paper.

Data availability

Data will be made available on request.

Acknowledgement

MM and MK contributed equally to preparation of the manuscript.

The National Research Council of Canada publication number 58356.

Appendix A. Supplementary data

Supplementary data to this article can be found online at https://doi.org/10.1016/j.yrtph.2023.105336.

References

Achenbach, J.C., et al., 2020. Comparison of the zebrafish embryo toxicity assay and the general and behavioral embryo toxicity assay as new approach methods for chemical screening. Toxics 8.
FastQC Andrews, S., 2010. A Quality Control Tool for High Throughput Sequence Data.
Baumann, L., et al., 2016. Thyroid disruption in zebrafish (Danio rerio) larvae: different molecular response patterns lead to impaired eye development and visual functions. Aquat. Toxicol. 172, 44–55.
Caballero, M.V., Candiracci, M., 2018. Zebrafish as Toxicological model for screening and recapitulate human diseases. Journal of Unexplored Medical Data 3.
Cassar, S., et al., 2019. Use of zebrafish in drug discovery toxicology. Chem. Res. Toxicol. 33, 95–118.
Cassar, S., et al., 2020. Zebrafish as an animal model for ocular toxicity testing: a review of ocular anatomy and functional assays. Toxicol. Pathol. 49, 438–454.
Corchete, L.A., et al., 2020. Systematic comparison and assessment of RNA-seq procedures for gene expression quantitative analysis. Sci. Rep. 10.
Davis, J.A., et al., 2011. Introduction to benchmark dose methods and U.S. EPA's benchmark dose software (BMDS) version 2.1.1. Toxicol. Appl. Pharmacol. 254, 181–191.
Dobin, A., et al., 2013. STAR: ultrafast universal RNA-seq aligner. Bioinformatics 29, 15–21.
Dobin, A., Gingeras, T.R., 2015. Mapping RNA-seq reads with STAR. Curr Protoc Bioinformatics 51, 11 14 1-11 14 19.
Dolgin, E., 2010. Animal testing alternatives come alive in US. Nat. Med. 16, 1348.
Farmahin, R., et al., 2017. Recommended approaches in the application of toxicogenomics to derive points of departure for chemical risk assessment. Arch. Toxicol. 91, 2045–2065.
Hahn, S., et al., 2006. Resorcinol. World Health Organization.
Hayes, A.W., et al., 2020. Dose and dose-response relationships in toxicology. Loomis's Essentials of Toxicology 17–31.
Izadi, H., et al., 2012. Evaluation of the benchmark dose for point of departure determination for a variety of chemical classes in applied regulatory settings. Risk Anal. 32, 830–835.
Jarque, S., et al., 2018. An automated screening method for detecting compounds with goitrogenic activity using transgenic zebrafish embryos. PLoS One 13, e0203087.
Johnson, K.J., et al., 2020. A rat liver transcriptomic point of departure predicts a prospective liver or non-liver apical point of departure. Toxicol. Sci. 176, 86–102.
Johnson, K.J., et al., 2022. A transformative vision for an omics-based regulatory chemical testing paradigm. Toxicol. Sci. 190, 127–132.
Jones, I., et al., 2003. The thyroid hormone receptor beta gene: structure and functions in the brain and sensory systems. Thyroid 13, 1057–1068.
Kanungo, J., et al., 2014. Zebrafish model in drug safety assessment. Curr. Pharmaceut. Des. 20, 5416–5429.
Kavlock, R.J., et al., 2018. Accelerating the pace of chemical risk assessment. Chem. Res. Toxicol. 31, 287–290.
Lai, K.P., et al., 2021. Zebrafish as the toxicant screening model: transgenic and omics approaches. Aquat. Toxicol. 234, 105813.
LaRocca, J., et al., 2020. Short-term toxicogenomics as an alternative approach to chronic in vivo studies for derivation of points of departure: a case study in the rat with a triazole fungicide. Regul. Toxicol. Pharmacol. 113, 104655.
Leist, M., et al., 2012. Novel technologies and an overall strategy to allow hazard assessment and risk prediction of chemicals, cosmetics, and drugs with animal-free methods. ALTEX 29, 373–388.
Love, M.I., et al., 2014. Moderated estimation of fold change and dispersion for RNA-seq data with DESeq2. Genome Biol. 15, 550.
Martin, M., 2011. Cutadapt removes adapter sequences from high-throughput sequencing reads. EMBnet J 17, 10–12.
OECD, 2020. Overview of Concepts and Available Guidance Related to Integrated Approaches to Testing and Assessment (IATA). OECD Series on Testing and Assessment, No. 329, Environment, Health and Safety. Environment Directorate, OECD.
Page-Lariviere, F., et al., 2019. Transcriptomic points-of-departure from short-term exposure studies are protective of chronic effects for fish exposed to estrogenic chemicals. Toxicol. Appl. Pharmacol. 378, 114634.
Phillips, J.R., et al., 2019. BMDExpress 2: enhanced transcriptomic dose-response analysis workflow. Bioinformatics 35, 1780–1782.
Reider, M., Connaughton, V.P., 2014. Effects of low-dose embryonic thyroid disruption and rearing temperature on the development of the eye and retina in zebrafish. Birth Defects Res B Dev Reprod Toxicol 101, 347–354.
Rodrigues, P., et al., 2020. Norfluoxetine and venlafaxine in zebrafish larvae: single and combined toxicity of two pharmaceutical products relevant for risk assessment. J. Hazard Mater. 400, 123171.
Scholz, S., et al., 2013. A European perspective on alternatives to animal testing for environmental hazard identification and risk assessment. Regul. Toxicol. Pharmacol. 67, 506–530.

Schuttler, A., et al., 2017. The transcriptome of the zebrafish embryo after chemical exposure: a meta-analysis. Toxicol. Sci. 157, 291–304.
Sukardi, H., et al., 2011. Zebrafish for drug toxicity screening: bridging the in vitro cell-based models and in vivo mammalian models. Expet Opin. Drug Metabol. Toxicol. 7, 579–589.
Thienpont, B., et al., 2011. Zebrafish eleutheroembryos provide a suitable vertebrate model for screening chemicals that impair thyroid hormone synthesis. Environ. Sci. Technol. 45, 7525–7532.
Van Norman, G.A., 2019. Limitations of animal studies for predicting toxicity in clinical trials: is it time to rethink our current approach? JACC Basic Transl Sci 4, 845–854.